ACS SyntheticBiology

Research Article

pubs.acs.org/synthbio

Biosensor-Based Evolution and Elucidation of a Biosynthetic Pathway in *Escherichia coli*

Yongfei Liu,[†,‡] Yinyin Zhuang,[†] Dongqin Ding,[†,‡] Yiran Xu,[†] Jibin Sun,[†,‡] and Dawei Zhang*[,†,‡]

[†]Tianjin Institute of Industrial Biotechnology, Chinese Academy of Sciences, Tianjin 300308, China

[‡]Key Laboratory of Systems Microbial Biotechnology, Chinese Academy of Sciences, Tianjin 300308, China

Supporting Information

ABSTRACT: The successful evolution of metabolite-producing microbes requires a high-throughput screening method to obtain the desired properties within a short time. In this study, we developed a transcription-factor-driven device that combines a metabolite-responsive element and a selection module. This device was able to specifically sense intracellular L-phenylalanine (L-Phe) and convert this signal into an observable phenotype. Applying this device, we successfully improved L-Phe production by screening hyperproducing phenotypes from a ribonucleotide binding site library and a random mutagenesis library. In addition, several site mutations introduced by random mutagenesis were identified and elucidated to facilitate the improvement of L-Phe production. Our results present a paradigm for screening of compounds that are not easily observable to raise the yield of targeted compounds from a large candidate library. This approach may guide further applications in rewiring metabolic circuits and facilitate the directed evolution of recombinant strains.

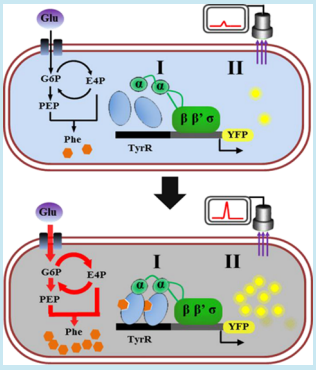

KEYWORDS: *biosensor, transcription factor, L-phenylalanine, high-throughput screening, TyrR*

Recently, much attention has focused on the recombination of microorganisms to produce small molecular compounds with great additional value.[1−5] Because conventional strategies do not always generate the desired levels of production as a result of incomplete information about the physiological and genetic background of the microorganisms, improving the yield of target products is often a daunting task. Compared with rational design approaches, a strategy that includes random mutagenesis by the creation of mutant libraries and high-throughput screening (HTS) may be more effective in finding and evolving phenotypes of interest.[6,7] However, only some conspicuous compounds can be accurately detected by conventional high-throughput colorimetric[8,9] and fluorometric assays,[10] and inconspicuous compounds without an obvious signature cannot be detected using current HTS technology.

Organisms take full advantage of the malleability of protein structure to employ macromolecules as reporters whose functional roles depend on the presence of specific ligand molecules. Inspired by these natural mechanisms, several natural molecular devices have been engineered to monitor inconspicuous small molecules *in vivo*.[7,11,12] One promising strategy is to utilize transcription factors (TFs) in a biosensor device for HTS of inconspicuous compounds.[13] In this strategy, effector molecules activate the transcription of a regulated gene, so the signal increases when the effector is exogenously added or endogenously generated. Thus, TFs can be used as biosensor tools to monitor the elevated concentration of small metabolites *in vivo*. *Escherichia coli* has more than 230 kinds of transcription factors, providing a comprehensive candidate pool to design biosensor tools to sense various metabolites.[14] To date, TFs have been applied to sense sugars, vitamins, antibiotics, amino acids, naringenin, benzoic acid-related compounds, triacetic acid lactone, malonyl-CoA, and acyl-CoA derivatives.[9,14−20] This strategy offers flexibility, as the effector of a particular TF can be switched to novel compounds by engineering the structural characteristics of the initial TF.[13,21−23] For example, AraC, a natural biosensor of L-arabinose, was successfully engineered to detect mevalonate and D-arabinose, and by the application of the designed system as a screening platform, mevalonate production was improved to 17 mM in *E. coli*.[21] Although the development of biosensor devices for detection of small molecules is of growing interest, few TFs have been adapted to compound measurement, and the sensitivity and dynamic range of those biosensors limit their further applications.

TyrP is a tyrosine-specific permease, and the *tyrP* promoter is activated by the TyrR protein in the presence of L-Phe.[24,25] In this study, we attempted to utilize this native regulatory device to monitor variations in the intracellular L-Phe concentration by detecting a TyrR-controlled reporter gene. By means of this strategy, an HTS platform with high sensitivity and wide dynamic range was established to facilitate the characterization, identification, and isolation of novel producers in high L-Phe yield. This method enabled us to obtain a large amount of novel phenotypes of interest from a mutant library in a short

Received: November 3, 2016
Published: January 25, 2017

DOI: 10.1021/acssynbio.6b00328
ACS Synth. Biol. 2017, 6, 837−848

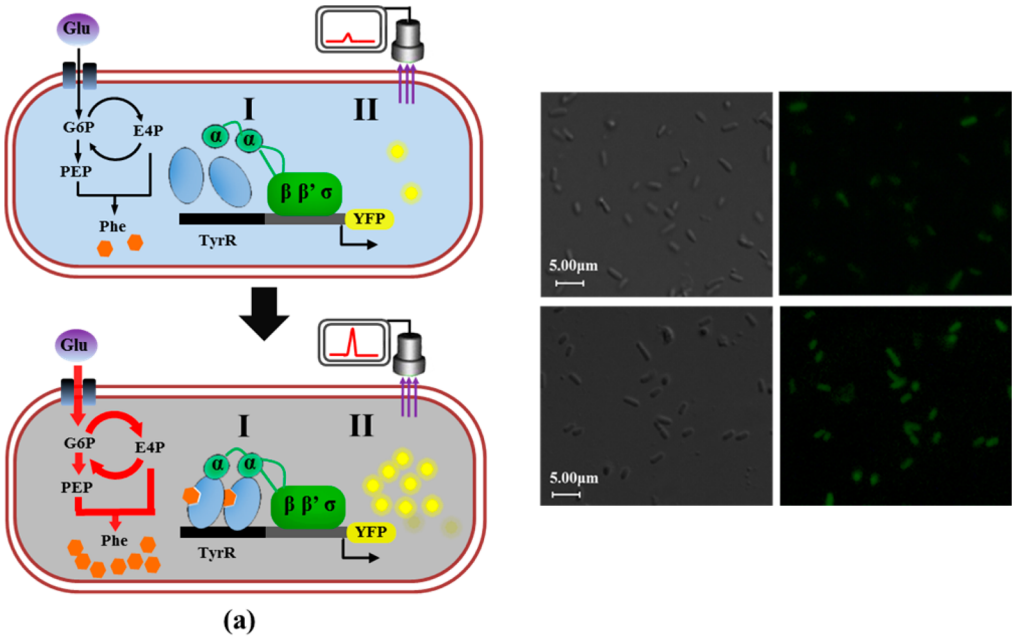

Figure 1. Design and characterization of the Phe-based biosensor. (a) Schematic diagram of the principle of the TF-driven biosensor. Cells with wild-type levels of effector amino acids present a background level of YFP fluorescence (upper panel). Increased intracellular concentrations of L-Phe could enhance the activation effect on the transcription level of P_{tyrP} and result in an increase in the YFP expression level in cells (lower panel). (b). Fluorescence microscopy images of cells carrying the pTF-TyrR1 sensor plasmid fed with 1 mM Phe-Phe dipeptide (lower row) and cells without dipeptides (upper row).

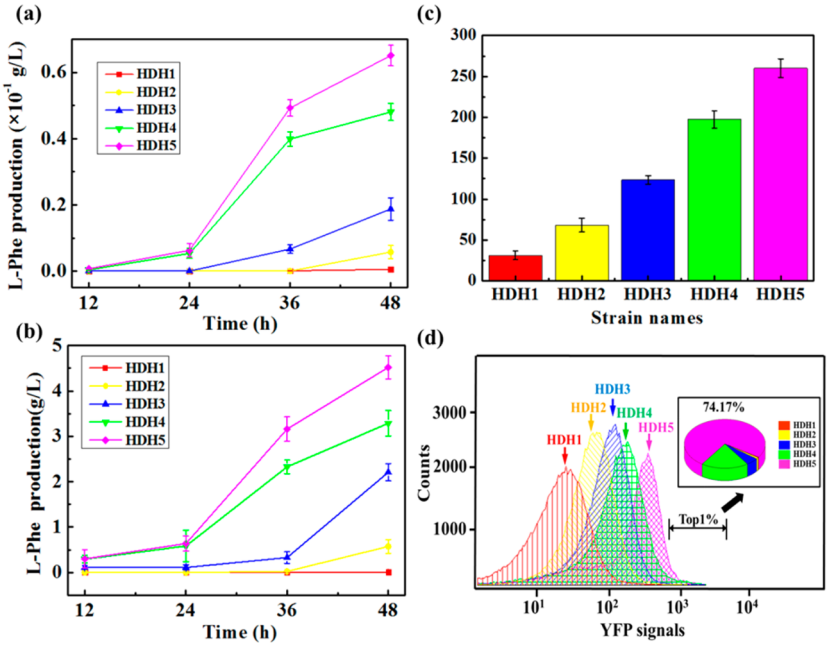

Figure 2. Characterization and validation of the L-Phe biosensor in Phe-hyperproducing recombinant strains. (a) Cytosolic L-Phe concentrations of five L-Phe producer strains. Different colors represent different strains. Error bars show the standard deviation of three independent cultures for each strain. (b) Extracellular concentrations of L-Phe produced by the five recombinant strains in (a). (c) Fluorescence values of the five defined strains in (a) carrying the pTF-TyrR1 sensor plasmid. (d) FACS results for the five strains mixed at equal OD. Strains exhibiting the top 1% of the fluorescence values were selected by FCM. The screened strains were then cultivated on agar plates at 37 °C overnight and distinguished by PCR.

period of time and provided insight into the complex regulation of the L-Phe biosynthesis pathway in *E. coli*.

RESULTS

Design and Characterization of a Novel L-Phe Biosensor. A schematic diagram of the biosensor designed in this experiment is presented in Figure 1a. This biosensor consists of two modules: a transcription factor device that activates the expression level of the downstream gene by the elevated concentration of ligand metabolites (module I in Figure 1a) and a reporter module that serves as a selecting marker to allow high-throughput screening (module II in Figure 1a). This biosensor can sense elevated concentrations of cytoplasmic L-Phe and activate the expression level of yellow

DOI: 10.1021/acssynbio.6b00328
ACS Synth. Biol. 2017, 6, 837−848

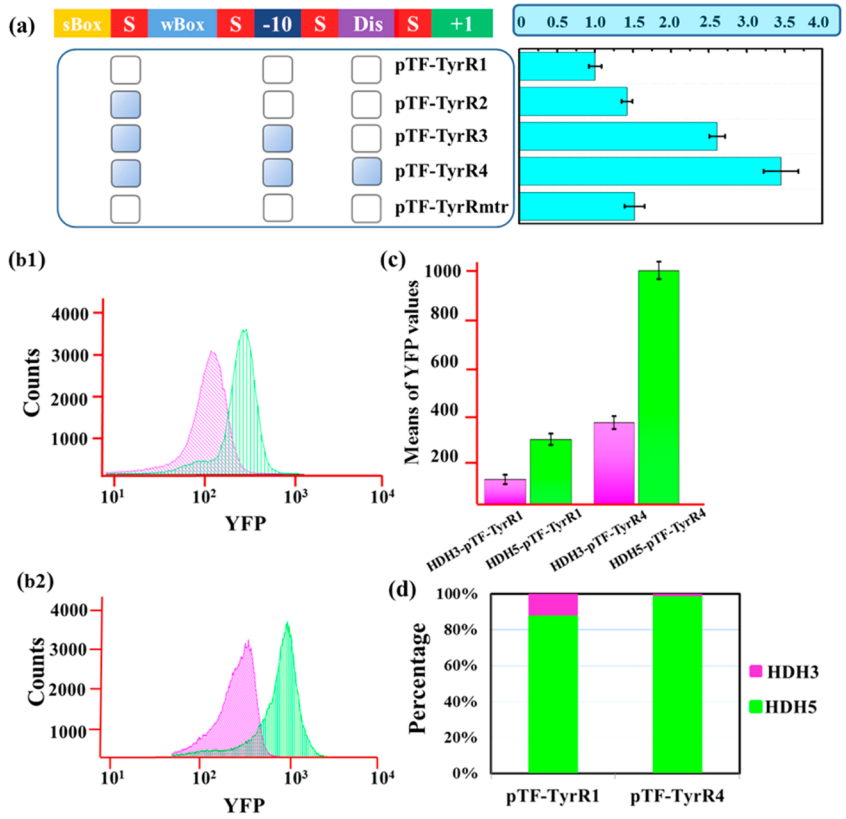

Figure 3. Optimization of TyrR-driven biosensors. (a) Effects of mutations in the *tyrP* promoter region on TyrR-mediated activation of P_{tyrP} and P_{mtr}. Three mutations were separately located in the space between the strong TyrR box and weak TyrR box, the −10 region, and the discriminator box of the *tyrP* promoter. Solid squares represent mutations that were introduced into the promoter sequence, and hollow squares represent unchanged sequence. (b) FACS results for two L-Phe producers (HDH3 and HDH5) using pTF-TyrR1 (b1) or pTF-TyrR4 (b2) as a screening tool. (c) Fluorescence values of HDH3 carrying pTF-TyrR1 or pTF-TyrR4 plasmid and HDH5 carrying pTF-TyrR1 or pTF-TyrR4. (d) Differentiation of the population distribution of an equal mixture of cells of two L-Phe producers by using pTF-TyrR1 or pTF-TyrR4 as a screening tool. After sorting by FCM, cells were cultivated on agar plates, and PCR analysis was carried out to distinguish the two L-Phe producers.

fluorescent protein (YFP), which is detectable by flow cytometry. By applying a dipeptide feeding assay, we artificially altered the concentrations of intracellular L-Phe in *E. coli* DH5α to confirm the function of this device. In view of the strict regulation of the amino acid transport systems in *E. coli*, this assay provided a more effective way to improve the cytoplasmic L-Phe level.[26] When dipeptides were added to the medium, the peptides underwent active uptake through the peptide transport systems and subsequent hydrolysis by cytoplasmic hydrolases, which improved the intracellular L-Phe level and consequently provided an appropriate substrate to activate the promoter.

When 1 mM Phe-Phe dipeptide was added to the medium, a clear difference in YFP fluorescence strength was observed in *E. coli* DH5α cells carrying the pTF-TyrR1 sensor plasmid (Figure 1b). This indicated that the sensor system was sensitive to the elevated intracellular L-Phe concentrations and was capable of reflecting this concentration difference by altered fluorescence intensity. Samples without Phe-Phe showed a detectable fluorescence value, which was attributed to the leaky expression of YFP under the control of P_{tyrP}. Moreover, there was a corresponding rise in YFP fluorescence of *E. coli* DH5α cells with increasing Phe-Phe dipeptide concentration (Figure S1a). The well-behaved characteristics of this device suggest its utility as a screening platform for selecting hyperproducing strains from a large, physiologically diverse bacteria library.

Biosensor Response to Extracellular L-Phe. We next investigated the correlation between the responsive fluorescence signal and the intracellular L-Phe concentration to confirm the feasibility of this biosensor. The pTF-TyrR1 sensor plasmid was transformed into HDH1 and four other defined mutants that exhibited increased L-Phe productivity (Table S1). The fluorescence value, optical density (OD), and L-Phe production of each strain were measured every 12 h. The growth conditions for the five strains were basically consistent (Figure S2). The intracellular L-Phe level of HDH1 remained under the limit of detection throughout the whole fermentation process. The other four defined producers began to accumulate L-Phe within 24 h and reached final cytosolic L-Phe concentrations ranging from 5.75 to 60.01 mg/L (Figure 2a). It was obvious that the concentration of extracellular L-Phe for the five strains showed a positive relationship with the intracellular L-Phe level (Figure 2b). The YFP fluorescence values of the five strains were detected by flow cytometry (FCM) at the end of the fermentation. As expected, there was an obvious increase in specific YFP fluorescence in going from HDH1 to HDH5 (Figure 2c,d). To evaluate the sorting performance of the pTF-TyrR1 sensor plasmid, we sorted colonies exhibiting the top 1% of the fluorescence values and identified the selected colonies by PCR analysis. As shown in Figure 2d, 74.17% of the sorted cells were identified as the HDH5 strain, indicating that this biosensor was able to effectively differentiate between different L-Phe producers and sort the hyperproducing strains with high efficiency.

DOI: 10.1021/acssynbio.6b00328
ACS Synth. Biol. 2017, 6, 837−848

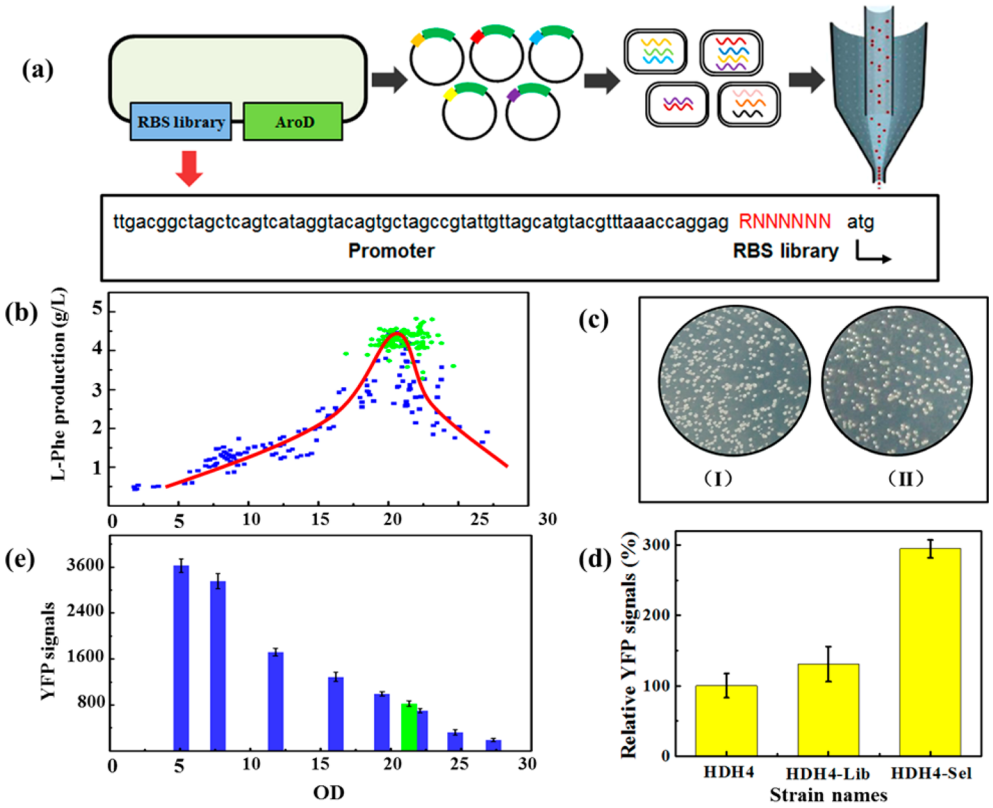

Figure 4. Optimization of the L-Phe biosynthetic pathway driven by the biosensor. (a) Flow diagram of the high-throughput screening experiment for selecting ideal phenotypes from an RBS library. The library was constructed in the pTrc99a vector by introducing seven random sequences in the RBS of *aroD* and then transformed into the HDH4 strain. After fermentation in a shake flask, strains were collected and treated by FACS analysis. (b) Fermentation results of FACS-selected colonies (green dots) and random-selected colonies (blue dots). (c) Comparison of phenotypes of random-selected colonies (I) and FACS-selected colonies (II). (d) Means of fluorescence values for HDH4, HDH4 carrying pTrc-aroD-lib, and strains selected from the RBS library. (e) Relative expression level of AroD in randomly selected strains (blue columns) and FACS-selected strains (green column).

Improving the Sensitivity and Dynamic Range of the Biosensors. Although TF-based fluorescence-activated cell sorting (FACS) allows ultrahigh throughput in cell sorting, one obvious disadvantage of this method is the overlapping fluorescence profiles, which reduce the sorting efficiency and have a high rate of false positives. One strategy to solve this problem is to amplify the output fluorescence signals that correspond to the specific metabolites. To test the feasibility of this idea, three novel sensor plasmids containing different site mutations in the TyrR regulation domain were constructed to evaluate the sorting efficiency.[27,28] As can be seen from Figure 3a, the strength of P_{tyrP} in pTF-TyrR2, pTF-TyrR3, and pTF-TyrR4 increased by 1.5-fold, 2.6-fold and 3.5-fold, respectively compared with pTF-TyrR1. Although TyrR showed stronger activation for P_{mtr} than P_{tyrP}, the strength of the artificial *tyrP* promoter was 2.3-fold higher than that of the *mtr* promoter when three site mutations were introduced into P_{tyrP}. The fluorescence values of strains carrying different biosensor plasmids in response to Phe-Phe are presented in Figure S1. Compared with pTF-TyrR1, the sensitivity and dynamic range of pTF-TyrR4 was significantly improved. Next, we selected two L-Phe producers, HDH3 and HDH5, to evaluate the FACS efficiency of the pTF-TyrR4 sensor plasmid. Strain HDH3 carrying pTF-TyrR1 or pTF-TyrR4 and strain HDH5 carrying pTF-TyrR1 or pTF-TyrR4 were fermented in flasks for 48 h in parallel. Strains carrying the same sensor plasmid were mixed at equal OD and then analyzed by FACS. Compared with pTF-TyrR1, the specific spectrograms of HDH3 and HDH5 were effectively separated by utilizing pTF-TyrR4 as a screening tool (Figure 3b). This might be explained by the obvious differences between the HDH3 and HDH5 strains when carrying plasmid pTF-TyrR4 (Figure 3c). After sorting by FCM, PCR analysis was carried out to distinguish HDH3 and HDH5. The proportion of HDH5 increased from 86.2% to 99.5% (Figure 3d) when pTF-TyrR4 was utilized as a screening tool in FACS, demonstrating that pTF-TyrR4 was a more sensitive biosensor for L-Phe and reduced the false-positive rate (the proportion of HDH3) in screening.

Biosensor-Driven L-Phe Synthetic Pathway Optimization. In our previous study, a quantitative proteomics approach with iTRAQ LC−MS/MS technologies was applied to investigate the metabolic flux in the HDH4 strain. The third step of the shikimate (SHIK) pathway, catalyzed by AroD, was demonstrated as the rate-limiting step for L-Phe production (unpublished data). Additionally, it is difficult to determine the optimized expression level of *aroD* to maximize the L-Phe production. To solve this problem, we constructed a ribonucleotide binding site (RBS) library with seven random nucleotides in the RBSs of *aroD* and screened for the ideal phenotype with optimal expression level of AroD (Figure 4a). A pool of pTrc99a-derivative plasmids carrying the RBS library was transformed into the HDH4 strain harboring pTF-TyrR4 plasmid. Strains that were not subjected to FACS were selected randomly and used as a control group. The FACS-selected and

DOI: 10.1021/acssynbio.6b00328
ACS Synth. Biol. 2017, 6, 837−848

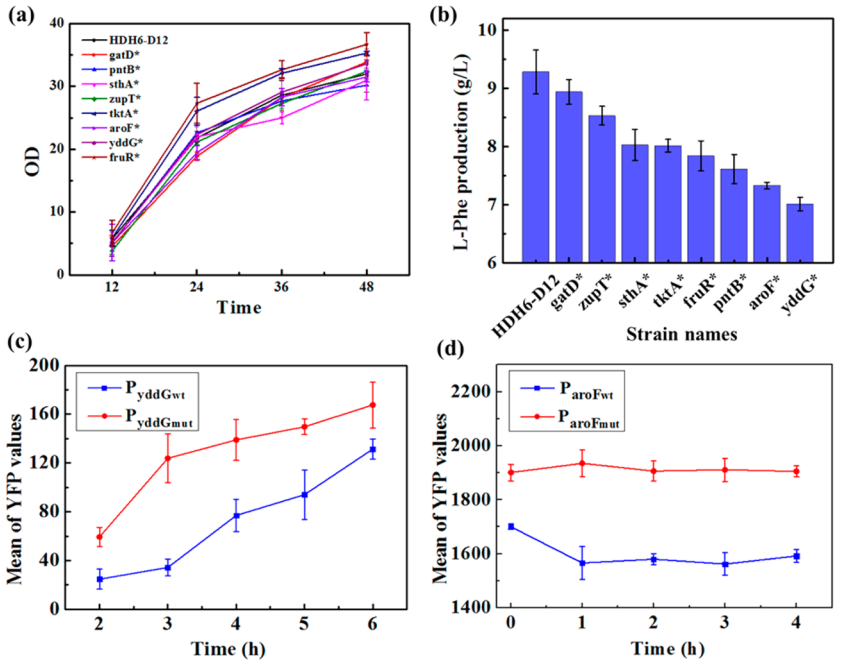

Figure 5. Fermentation results for HDH6-D12 and its derivative strains produced by back mutation. (a) Growth conditions of HDH6-D12 and eight derivative strains. An asterisk on the gene indicates that the strain was reconstructed by back mutation on that gene. (b) Fermentation results for HDH6-D12 and the eight derivative strains in (a). (c) Comparison of promoter strengths of $yddG_{wt}$ and $yddG_{mut}$. The promoters of $yddG_{wt}$ and $yddG_{mut}$ were separately ligated into pUC18 harboring YFP as a reporter. The YFP fluorescence values were detected every 1 h. (d) Comparison of promoter strengths of $aroF_{wt}$ and $aroF_{mut}$. Promoter sequences of $aroF_{wt}$ and $aroF_{mut}$ were cloned into pUC18 harboring YFP as a reporter. Fluorescence values were measured every 1 h.

randomly selected strains were separately cultivated in 96-well microplates. As expected, the growth rates of randomly selected cells showed significant variation due to the different expression levels of AroD. The L-Phe production peaked as the OD gradually increased to 22 but decreased when the biomass further increased (Figure 4b). We assumed that there was a trade-off between the accumulation of biomass and the production of target compounds in the bacteria. This is likely because as the expression level of AroD increased, excessive E4P and PEP entered the L-Phe synthesis pathway, and the carbon sources utilized for cell growth were drastically reduced. Also, a high concentration of intermediate metabolites accumulated in the L-Phe pathway and caused cell damage. In contrast, FACS-selected strains maintained a consistent growth rate (Figure 4b,c). The fluorescence value of strains harboring library plasmids was improved by 1.3-fold, and the FACS-selected strains significantly improved by 2.95-fold. (Figure 4d). Through sequencing, the optimal RBS sequence of *aroD* in the HDH4 strain was "ATATACT". The L-Phe production of the highest-producing strain was 5.79 g/L (HDH6), approximately 180% higher than the initial strain HDH4.

To further investigate the relationship between the expression level of AroD and L-Phe production by the HDH4 strain, we selected colonies with various growth rates to determine the expression levels of AroD. GFP was positioned downstream of the RBS of *aroD* as a reporter. As shown in Figure 4e, the L-Phe production showed a parabolic correlation with varying AroD flux. This verified our assumption that an excessive level of AroD caused a metabolic burden for cell growth, which ultimately lowered the L-Phe production. Our results were in an agreement with a previous study on predicted flux distributions responding to varying *ppc* flux in *E. coli*.[29] These results demonstrated that the strains with the optimal *aroD* expression level for L-Phe production could be effectively enriched and sorted from a large pool of candidates with the biosensor plasmid.

Use of the Biosensor To Screen Hyperproducing Strains from a Random Mutagenesis Library. We next investigated the feasibility of the sensor for screening hyperproducing strains from a random mutagenesis library. FACS is widely used because of its ultrahigh efficiency, but overlapping fluorescence profiles and anomalous fluorescence *in vivo* due to the heterogeneity of cells during different growth periods may complicate the interpretation of FACS results. To avoid this problem, we used plate-based resistance screening. Compared with the instantaneous detection by FCM, screening on agar plates is a longer process that can effectively minimize the eventuality of an anomaly. To do this, we substituted YFP with the resistance gene *strA* as a selection marker for HTS. The feasibility and practicality of this novel reporter were confirmed by the agar-plate screening test (Figures S3 and S4). In order to obtain a genome-wide perturbation mutant library, HDH6 strains were treated with atmospheric and room-temperature plasma (ARPT) according to the operation manual. For the first step of screening, we cultivated the mutants on the agar plate containing 50 μg/mL streptomycin after mutagenesis by ARPT. For the second screening step, we applied a rapid fluorescence measurement method to detect the L-Phe concentrations in 96-well microtiter plate broth.[30] The accuracy of the optimized method was evaluated by comparing the fluorescence results and HPLC results (Agilent 1260) (Figure S5). In a parallel control, colonies grown without streptomycin selection were cultured under the same conditions for comparison.

As shown in Figure S6, after four rounds of mutagenesis by ARTP and agar-plate screening, a total of 378 colonies were

DOI: 10.1021/acssynbio.6b00328
ACS Synth. Biol. 2017, 6, 837−848

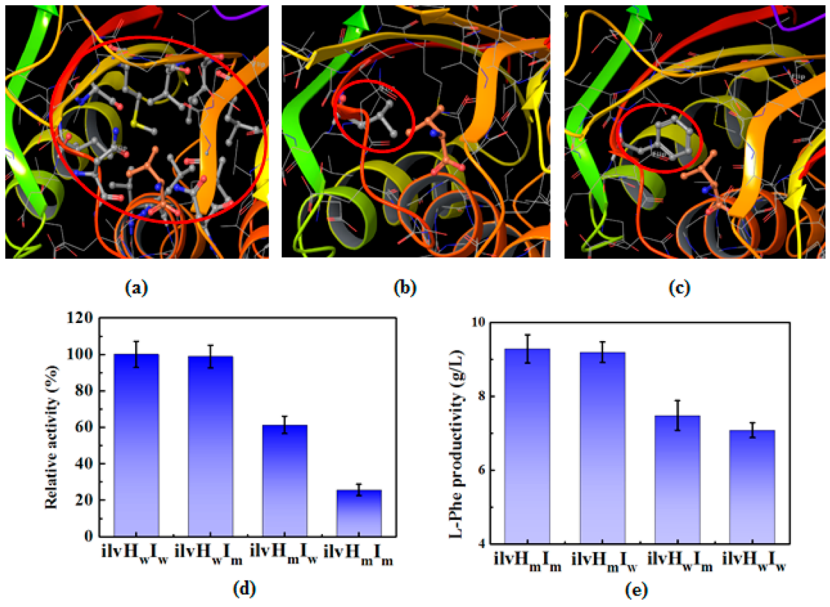

Figure 6. Relative activities of wild-type and mutant AHAS and the impact of mutation on L-Phe production. (a) Schematic diagram of suggested effector sites for binding pyruvic acid (marked with the red ellipse). This diagram is based on the published structures of AHAS from the Protein Data Bank (http://www.rcsb.org/pdb/home/home.do). All of the images were generated using the UCFS Chimera software. (b) Schematic diagram of the wild-type nonpolar side chains of Leu9. (c) Schematic diagram of the mutant nonpolar side chains of Phe9. (d) Relative activities of wild-type and mutant AHAS containing $ilvH_m$ or $ilvI_m$. (e) Fermentation results for HDH6-D12 and its three defined mutants. All of the fermentation experiments were carried out in triplicate.

selected from the random mutagenesis library. After fermentation in 96-well microtiter plates, around 68.9% (262/380) of the mutants produced higher L-Phe than the initial strain and less than 2% (6/380) of the colonies in the control group showed higher L-Phe production. The highest production of the selected strain (HDH6-D12) was 9.29 g/L, an increase in L-Phe production of 160.2% relative to the parental strain HDH6. These results confirmed that this biosensor system substantially simplified the process, shortened the screening period, and ultimately increased the positive rate of the high-throughput selection.

Elucidation of Evolved Enzyme in the L-Phe Biosynthesis Pathway. For a strain with enhanced metabolic flux toward targeted compounds, the evolution of enzymes involved in the synthesis pathway is a key step because improved enzyme activity could increase the supply of the intermediate metabolite and ultimately improve the productivity of targeted compounds. Thus, we performed whole-genome sequencing on the HDH6-D12 strain, which was the highest-yielding strain selected from the genomic library. The results showed that a total of 41 single-nucleotide polymorphisms (SNPs) were observed in the genome of HDH6-D12 (their sequences are shown in Table S4). To elucidate the high-yield mechanism for the HDH6-D12 strain, we reconstructed a series of strains derived from HDH6-D12 by introducing individual back mutations into the chromosome. The back-mutation experiment was performed using CRISPR-Cas9-mediated genome editing as described by Zhao.[31]

As illustrated in Figure 5b, the specific mutation in *tktA* (A524T) caused a decrease in L-Phe productivity from 9.28 to 8.01 g/L. One possible explanation is that the decreased enzyme activity in TktA decreased the amount of intracellular E4P. SNPs in *pntB* (A167T) and *sthA* (A145 V) also showed direct contributions to the improvement of L-Phe production in HDH6-D12. The L-Phe production of the HDH6-D12-pntB* and HDH6-D12-sthA* strains decreased to 7.61 and 7.32 g/L respectively. We speculate that the increased activities of mutant SthA and PntB promoted the conversion from NADH to NADPH, which was necessary but insufficient for the L-Phe biosynthesis pathway in recombinant strains.[32] Overexpression of *sthA* or *pntAB* has been widely applied in recombined bacteria for producing NADPH-dependent compounds.[33,34] In addition, the back mutations of *gatD* (E308*) and *zupT* (W38*) resulted in losses of 5.1% and 9.4% in L-Phe production, respectively.

Of particular interest were SNPs in acetohydroxy acid synthase (AHAS), the first common enzyme in the branched-chain amino acid biosynthesis pathway, and encoded by ilvH and ilvI (*ilvH* L9F and *ilvI* A82 V). The SNP in *ilvH* is located in the putative effector binding site at the interface between the two ferredoxin-like domains, near the interface between the N-terminal domains of the two chains that forms the regulatory domain. The nonpolar valine side chain fit into a hydrophobic pocket formed by Leu9, Leu16, Val35, and other residues.[35,36] A schematic diagram of the proposed location of the substrate-binding site on *ilvH* was simulated using the UCFS Chimera software (Figure 6a). We predicted that the replacement of Leu9 with a Phe residue would increase the pyruvic acid resistance because the large volume of Phe would prevent substrate binding in the pocket (Figure 6b,c). Not surprisingly, the enzyme activities of ilvH$_m$I$_m$ and ilvH$_m$I$_w$ dramatically declined to 24.2% and 61.3% compared with ilvH$_w$I$_w$ (Figure 6d). The L-Phe production also decreased when ilvH$_w$ was used in place of ilvH$_m$ (Figure 6e). We speculate that the SNP in *ilvH* interfered with the binding of the substrate to the effector site of AHAS because of the larger volume of the Phe residue, resulting in a decrease in the enzyme activity of AHAS. The mutated enzyme subsequently reduced the consumption of intracellular pyruvate by weakening the reaction of pyruvate in the branched-chain amino acid pathway and consequently

DOI: 10.1021/acssynbio.6b00328
ACS Synth. Biol. 2017, 6, 837−848

limited the consumption of PEP to form pyruvate and increased the amount of PEP available for L-Phe synthesis *in vivo*.

Altering the Transcription Level of Key Enzymes To Improve L-Phe Production. Notably, one SNP was found in the promoter region of *yddG*, encoding an aromatic amino acid exporter protein. To determine whether this mutation was able to improve L-Phe secretion, we separately cloned the mutant and wild-type promoter sequences into pUC18 harboring *yfp* as a reporter (Figure S7). As shown in Figure 5c, the mutant's promoter showed higher activity than that of the wild type within 6 h, indicating that HDH6-D12 was able to effectively excrete intracellular L-Phe to the broth during fermentation.[37] Another point mutation was located at the third TyrR box in the promoter region of *aorF*.[24] As can be seen from Figure 5d, the promoter strength of $aroF_{mut}$ was roughly 1.4 times higher than that of $aroF_{wt}$ when 2 mM Tyr was added to the medium. This mutant TyrR box was confirmed to remove the feedback inhibition by TyrR in the presence of Tyr (Figure 5d). The expression level of the mutant was 1.3 times higher than that of the wild type, indicating a higher carbon flux toward the L-Phe synthesis pathway in HDH6-D12.

One particular phenomenon we observed was that HDH6-D12 exhibited slower glucose consumption in a 5 L fermenter compared with the HDH6 strain (data not shown). This may have improved the productivity of L-Phe because a low rate of glucose uptake could efficiently avoid the surplus PEP pouring into the TCA cycle. Since no SNP was found in the *pts* (phosphoenolpyruvate: carbohydrate phosphotransferase system) operon, we assumed that the SNP in the transcriptional regulator FruR (E173K) enhanced the repression of *pts* operon transcription. To test this hypothesis, we constructed the *fruR* gene back mutant, HDH6-D12-fruR*. The L-Phe production of HDH6-D12-fruR* was reduced by 15.7% compared with that of HDH6-D12 (Figure 5b), and the OD of this mutant was even higher than of HDH6-D12 (Figure 5a). To further verify the effect of *fruR*, we used an *E. coli* strain with the chromosomal *fruR* gene deleted, BW25113 ΔfurR, transformed with pTrc99a plasmids overexpressing $fruR_{wt}$ and $fruR_{mut}$ to produce BWFruR and BWFruRM, respectively (Figure S8). The transcription levels of *ptsG*, *ptsH*, *ptsI*, and *crr* in BWFruRM showed a dramatic decline compared with the transcription level in the BWFruR strain as measured by real-time PCR analysis (Figure 7). These changes in the transcription level of the *pts* operon are likely responsible for the observed low rate of glucose consumption during fermentation.

Overall, this biosensor tool enabled us to elucidate the mechanism in four aspects of the pathway to achieve high-yield production: (1) the evolution of key enzymes, (2) moderate attenuation of the branch pathway, (3) enhancing the transcription level of key enzymes, and (4) engineering the regulation function of a global transcription factor. As shown in Figure 8, in addition to the SNPs that improved L-Phe production (red bold italic), several other SNPs had potential impacts on L-Phe formation (black bold italic). These genes were involved in the following metabolic processes: ion channel proteins (*amtB* and *clcB*), phosphotransferase systems (*srlE*, *mtlA*, and *ompR*), ABC transporter systems (*proW*, *sgcC*, and *malK*), the central metabolic pathway (*mqo*, *aceA*, *aceK*, and *pykA*), stress-tolerant proteins (*phoQ*, *mtlD*, *phoR*, *degQ*, and *yhjA*), protein secretion (*gspC* and *gspJ*), and physiological-related proteins (*ftsI*, *efP*, and *flhD*). We inferred that these SNPs might play multiple functions in reducing the consumption rate of glucose to improve productivity, secreting cytoplasmic L-Phe into the culture medium, or assisting the strains to survive in the harsh fermentation environment containing high-titer products and other harmful intermediates or byproducts. A better understanding of the regulatory mechanisms of the overproducing strains requires future research.

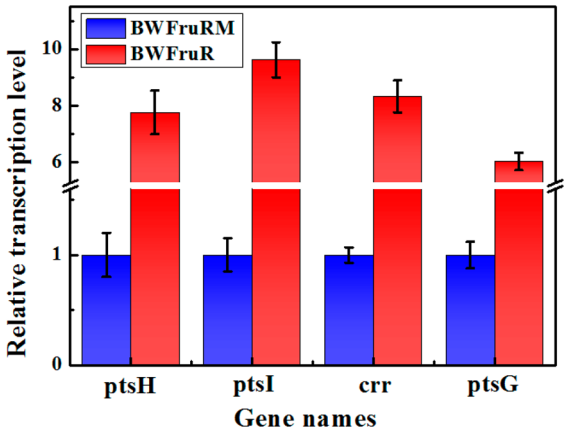

Figure 7. Relative transcription level of *pts* operon genes in BWFruR and BWFruRM as determined by real-time PCR. Experiments were conducted in triplicate, and measurements are represented as means with their standard deviation.

DISCUSSION

Organisms have evolved varied sensors to bind small cytoplasmic molecules. Among these devices, transcription-factor-driven biosensors have wide application in metabolic engineering to optimize synthetic pathways, reshape phenotypes, and reprogram cellular behaviors.[38−40] These devices offer many advantages. First, the small ligand molecules of a certain transcription factor are highly specific to a specific promoter, so the rate of false positives in the HTS can be maintained at a low level. Second, the TF−promoter pair allows *in vivo* detection of the target compounds, which eliminates the need for any *in vitro* manipulation. Third, the sensitivity of the TF biosensors is fairly comparable to that of NMR spectroscopy.[6] Because of the hypersensitivity and specificity of the TF-based biosensor, various genetic devices have been applied to optimize the synthetic pathway and predict the potential bottlenecks of targeted metabolites.[14,16,41] However, few efforts to improve the sensitivity and response range of these natural biosensors have been made. In this study, we created a synthetic TF−promoter pair biosensor, the sensitivity and dynamic range of which were significantly improved relative to those of the original module. Applying this device as a screening platform, we successfully improved the titer of L-Phe by optimizing the expression level of a key enzyme in the L-Phe biosynthesis pathway (Figure 4). In addition, we also investigated the applicability of this biosensor by screening high L-Phe producers from a random mutagenesis library. Our results clearly demonstrated that this novel Phe-responsive device functioned as an efficient screening tool for the improvement of L-Phe production in *E. coli*.

An important parameter describing the performance of biosensors is the apparent hill (N_{app}),[21] which is used to describe the sensitivity of sensors. According to the definition of N_{app}, a stronger activation effect of the TF−promoter pair

DOI: 10.1021/acssynbio.6b00328
ACS Synth. Biol. 2017, 6, 837−848

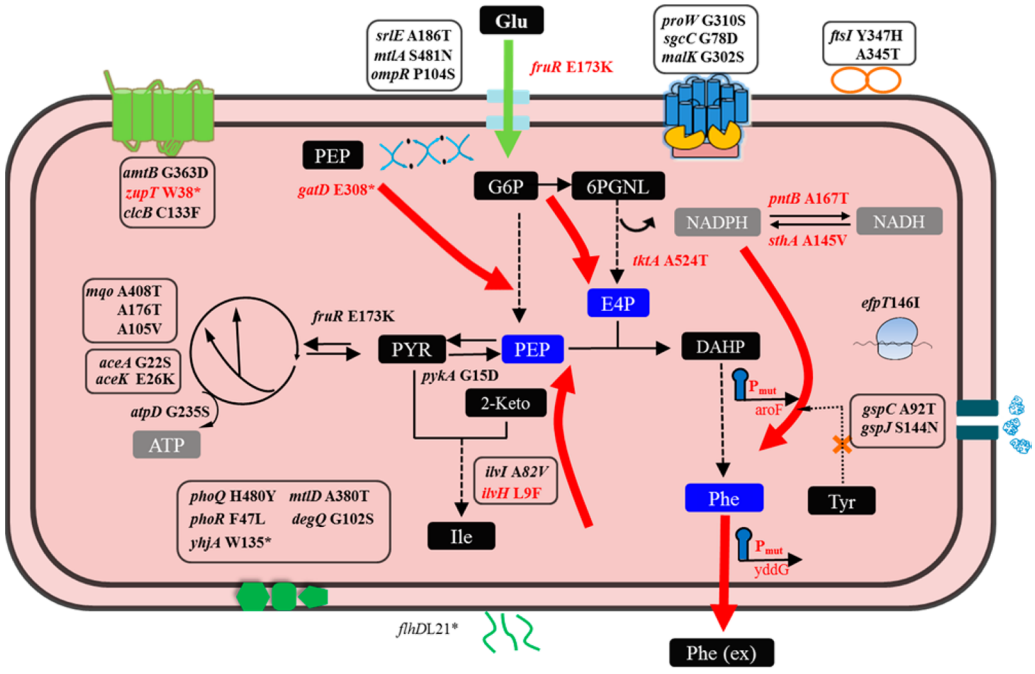

Figure 8. System-wide interpretation of the high-yield mechanism for the HDH6-D12 strain with the implementation of SNPs introduced by random mutagenesis. SNPs that were demonstrated to facilitate the improvement of L-Phe production are shown in red bold italic, and SNPs with a potential impact to improve L-Phe production are shown in black bold italic. Thick red arrows indicate that the metabolic flux was increased, while the thick green arrow indicates that the metabolic flux was decreased in HDH6-D12. Abbreviations: Glu, glucose; PEP, phosphoenolpyruvic acid; G6P, glucose-6-phosphate; 6PGNL, 6-phospho D-glucono-1,5-lactone; E4P, erythrose-4-phosphate; PYR, pyruvic acid; DAHP, 5-enolpyruvoyl shikimate 3-phosphate; Tyr, tyrosine; Phe, phenylalanine; Ile, isoleucine.

results in greater sensitivity and a wider range. TyrR activates both *tyrP* and *mtr* in the presence of L-Phe, and TyrR showed a stronger activation effect on P_{mtr} than P_{tyrP}.[24] However, pTF-TyrR4 was chosen as the optimal biosensor in the HT screening because of its higher signal response toward L-Phe. As shown in Figure S1, the sensitivity of pTF-TyrR4 was nearly 15 times higher than pTF-TyrR1. The detection threshold of pTF-TyrR4 was 0.1 mM Phe-Phe, but 1 mM Phe-Phe was required for pTF-TyrR1. These differences explain why a higher positive rate was obtained in the high-throughput screening using pTF-TyrR4 (Figure 3d).

Although some progress has been made to increase production of L-Phe in *E. coli*,[41−44] targeted modifications to improve the production have shown only moderate success for the isolation of high-yielding recombinant strains. By using biosensors in an HT screening, we were able to obtain a myriad of cells presenting increased intracellular concentrations of the effector amino acid. Compared with conventional strategies such as overexpressing or knocking out targeted genes in *E. coli*, the SNPs identified in our study were confirmed to play a key role in the hyperproduction. To our knowledge, the SNPs in *aroF*, *yddG*, *ilvH*, *tktA*, *sthA*, *pntB*, and *fruR* were not previously reported to improve L-Phe production in *E. coli*. These SNPs functioned by altering transcription levels and enzyme activities and enhanced the metabolic flux toward L-Phe generation. In addition, several unknown SNPs merit further research. For instance, an interesting phenomenon was observed in an analysis of the metabolic perturbation of HDH6-D12 by the addition of surplus L-Phe to the medium. We observed that most of the genes involved in the L-Phe synthesis pathway were abnormally upregulated as the concentration of L-Phe increased (Figure S9). In addition to TyrR, it has been reported that the L-Phe biosynthetic pathway could be regulated by the CpxA/CpxR transcriptional regulator, leucine-responsive regulatory protein,[45] and the CRP-cAMP DNA-binding transcriptional dual regulator.[46,47] Since no variation was found in these transcriptional regulators, we assume that the other SNPs that were not identified may be responsible for this phenomenon.

METHODS

Bacterial Strains, Plasmids, and Cultivation Medium. The *E. coli* strains and plasmids used in the study are listed in Table S1. Strain HDH1 was derived from *E. coli* W3110 and stored in our lab.[48] *E. coli* strains DH5a and BL21 (Transgene, Beijing) were used for cloning and expression. The pET28a plasmid was used to express and purify the proteins for analysis of enzymatic activities. The pTrc99a plasmid was used to overexpress the genes involved in L-Phe producers. The pREDCas9 plasmid was a kind gift of Xueming Zhao (Tianjin University, China) and was used for genome editing in *E. coli*. The pSenlys plasmid was a kind gift of Lothar Eggeling (Forschungszentrum Jülich GmbH, Germany) and was employed for the construction of the L-Phe biosensors reported here.

Individual colonies were cultivated in 500 μL of LB medium overnight in 96-well deep-well assay blocks (Corning Costar 3960, square V-bottom, 2 mL) and subsequently incubated in 500 μL of fermentation medium (20 g/L glucose, 10 g/L $(NH_4)_2SO_4$, 5 g/L KH_2PO_4, 5 g/L $MgSO_4$, 4 g/L yeast extract, 15 mg/L $FeSO_4{\cdot}7H_2O$, 15 mg/L $MnSO_4{\cdot}H_2O$, and 1 g/L betaine monohydrate) at 37 °C, 900*g*, 80% humidity for 48 h in a Microtron shaker (Infors, China). For shake flask fermentation, a colony selected from the agar plate was inoculated in LB medium overnight and then transferred into a 500 mL flask containing 20 mL of fermentation medium for 48 h at 37 °C. For cultivating strains in a 5 L fermenter (BioFlo/

DOI: 10.1021/acssynbio.6b00328
ACS Synth. Biol. 2017, 6, 837−848

CelliGen 310, Eppendorf, Germany), strains that were cultivated in LB medium overnight were inoculated into the seed culture (20 g/L glucose, 10 g/L $(NH_4)_2SO_4$, 1.5 g/L KH_2PO_4, 5 g/L $MgSO_4$, 4 g/L yeast extract, 15 mg/L $FeSO_4 \cdot 7H_2O$, 0.5 g/L sodium citrate, and 100 mg/L VB1, 1:50 v/v) for 7 h at 37 °C and then inoculated into a 5 L fermenter containing 3.5 L of culture (1:10 v/v). During batch-phase fermentation, the pH was maintained at 7.0 with 10% NH_4OH solution. The temperature was initially set at 33 °C and then increased to 38 °C when the OD_{600} reached 30 to induce the expression of key enzymes in the plasmid. The dissolved oxygen gradually decreased to 40% and was kept constant by cascading the aeration rate from 5 to 20 vvm (air volume/culture volume/min) and the agitation speed. When the initial glucose in the medium was exhausted, glucose feeding was performed using a peristaltic pump. Samples were collected every 2 h to determine the OD, the residual glucose, and the concentration of L-Phe.

Design and Optimization of Biosensors. Recombinant DNA procedures, including PCR, digestion, and ligation, were performed according to standard protocols. For construction of pTF-TyrR1, the *tyrR* gene, the first 200 nucleotides of *tyrP*, and the promoter of *tyrP* were amplified and ligated into pSenlys. For construction of pTF-TyrR2, three nucleotides were inserted between the strong TyrR box and weak TyrR box in the *tyrP* promoter on pTF-TyrR1. pTF-TyrR3 was obtained by introducing a site mutation in the −10 region of the *tyrP* promoter on pTF-TyrR2. Three nucleotides were changed from GCC to ATA in the discriminator sequence of *tyrP* promoter in pTF-TyrR3, creating pTF-TyrR4. The detailed sequences of the four biosensor plasmids are listed in Table S3.

Dipeptide Feeding Assay. A single colony was inoculated into LB medium and grown at 37 °C overnight. Cells were washed twice with PBS and inoculated into fresh M9 medium in 96-well plates. The dipeptide feed assay allowed the assay of peptide uptake and amino acid excretion and was initiated by addition of Phe-Phe to the medium. Cells were collected in the next 30 min and resuspended in cold PBS solution. The fluorescence value was measured by flow cytometry (FCM) (MoFlo XDP, Beckman, USA) and used to detect intracellular L-Phe concentration as described below.

Preparation of Cell Extracts To Detect Intracellular L-Phe Concentration. To prepare cell extracts, 500 μL of cell suspension was precipitated by centrifugation in a tube containing 100 μL of silicone oil. After disruption by sonication, cell pellets were resuspended in 200 μL of perchloric acid (20% v/v) by gentle vortexing. Extracts were neutralized by addition of 200 μL of Na_2CO_3 to remove membrane materials and denatured proteins by centrifugation. The supernatant was subsequently filtered through a filter membrane (0.22 μm) and stored at −20 °C. HPLC analysis was carried out according to the manufacturer's protocol.

Determination of L-Phe Production in 96-Well Microtiter Plates. L-Phe production in fermentation broth was measured by the optimized fluorescence assay.[30] L-Phe interacts with the ninhydrin in the acid solution containing certain dipeptides, and the fluorescence is enhanced and stabilized by Cu^{2+}. After cultivation in a 96-well deep-well assay block, cells were centrifuged at 10000*g* for 1 min. Next, 50 μL of supernatant was transferred to a new 96-well microtiter plate containing 50 μL of succinic acid buffer (0.3 M, pH 5.8), 150 μL of ninhydrin (30 mM), and 50 μL of Gly-Ile (5 mM). After reaction at 60 °C for 2 h, 40 μL of Cu^{2+} stabilizer (160 g/L Na_2CO_3, 6.5 g/L $C_4O_6H_4KNa$, and 6 g/L $CuSO_4$) was added to the solution to enhance the fluorescence. The fluorescence was measured by a microplate reader system (HITACHI).

Generation of the Synthetic RBS Library. The synthetic promoter library was generated using degenerate primers, in which "N" represents a random nucleotide (c/g/a/t) and "R" represents "a" or "g". The primer sequences are as follows: aroD-LF (5′- CCG ***GAATTC*** TTGACAAGAGATAA-CAACGTTGATATAATTGAGCC CGTATTGTTAGCATG-TACGTTTAAAC CAGGAGRNNNNNN ATGAAAACCG-TAACTGTAAAAGATCT); aroD-LR (CCG *GGTACC* TTATGCCTGGTGTAAAATAGTTAAT). The *aroD* gene was amplified from the *E. coli* K-12 genome using these primers and subsequently inserted into the pTrc99a vector to produce *pTrc- aroD-lib*. The plasmid library was then transformed into HDH4 strain and sorted by FCM. The top 1% of strains exhibiting the highest fluorescence were collected in a 96-well microtiter plate. Additionally, colonies were selected randomly from the library and served as comparisons.

Construction of the Random Mutagenesis Library and High-Throughput Screening. In order to screen the mutants on solid media, the reporter gene on pTF-TyrR4 was first replaced by *strA* conferring streptomycin resistance, affording pTF-TyrR5. The HDH6 strain carrying pTF-TyrR5 was cultivated in LB medium overnight and inoculated into fresh LB medium at a ratio of 1:200. Cells were grown until the OD_{600} reached 1.0, and then the cells were centrifuged and resuspended in PBS. The suspension was treated with an atmospheric and room-temperature plasma (ARTP) biological mutagenesis system (ARTP-II, Beijing) according to the provided manufacturer's instructions. The agar-plate screening was performed as follows: First, the optimized mutation time of the HDH6 strain was determined with the criterion that the mortality was roughly 90%. The range of the mutation time was from 10 to 20 s, and the mutation time was set within every 1 s. Second, the mutants were then cultivated on agar plates containing a wide range of streptomycin concentrations (from 0 to 60 μg/mL), and the optimal concentration of streptomycin was determined with the standard that the mortality was over 99%. More briefly, fewer than 50 colonies grew on the agar plates when approximately 5000 mutants were cultivated. The colonies that survived on the plate were fermented in a 96-well microtiter plate, and the L-Phe production was measured by the fluorescence assay.

Construction of Back Mutants of HDH6-D12 by CRISPR-Cas9-Mediated Genome Editing. The back-mutation experiment was operated according to the CRISPR-Cas9-mediated genome editing assay previously reported by Zhao.[31] Taking the back mutant of *ilvI* as an example, the 20 spacer sequence for the *ilvI* gene was synthesized in the primer Cas-ilvI-N20-LF and Cas-ilvI-N20-LR. To construct the gRNA plasmid pCas-ilvI, a PCR product was obtained by amplification of pREDCas9 using the primers Cas-ilvI-N20-LF and Cas-ilvI-N20-LR, transformed into *E. coli* DH5α, and cultivated at 30 °C overnight. The positive clones were selected and verified by PCR and DNA sequencing. To construct the double-strand donor DNA (dsDNA), two homologous arms were separately amplified and were fused together by fusion PCR. This dsDNA contained two site mutations, the back-mutation site of *ilvI* and a synonymous mutation in the "NGG" PAM sequence so the recombinant strains were not killed by Cas9-mediated digestion and no new SAP was introduced into the genome. A

DOI: 10.1021/acssynbio.6b00328
ACS Synth. Biol. 2017, 6, 837−848

diagrammatic sketch of the primers for dsRNA is shown in Figure S10.

gRNA plasmid (100 ng) and donor dsDNA (100 ng) were transformed into electrocompetent cells, and the electroporation parameters were 0.1 cm cuvette and 1.70 kV (Bio-Rad MicroPulser). Cells after electroporation were cultivated in 1 mL of LB medium for 2 h prior to plating on LB plates containing 0.2% arabinose overnight. To improve the editing efficiency, colonies that survived on the agar plate were then recultivated in LB plates containing 0.2% arabinose. Strains that survived were selected and verified by PCR and DNA sequencing. The primers used in this study are listed in Table S2.

Construction of Plasmids for Verifying the Function of SNPs. To construct the plasmids pUC18-yddG$_{wt}$ and pUC18-yddG$_{mut}$, the promoters accompanying the first 120 base pairs of *yddG*$_{wt}$ and *yddG*$_{mut}$ were separately amplified from the genome of *E. coli* W3110 and HDH6-D12, and the *yfp* gene was amplified from pSenlys. The gene fragments were then fused with the *yfp* gene by fusion PCR. Next, the pUC18 plasmid and the PCR fragments were digested by *Sal*I and *Bam*HI and ligated by T4 ligase at room temperature for 3 h. The plasmid profile of pUC18-yddG$_{mut}$ was the same as that of pUC18-yddG$_{wt}$ except for the introduction of the site mutation in the *yddG* gene. The construction of pUC18-aroF$_{wt}$ and pUC18-aroF$_{mut}$ was the same as that of pUC18-yddG$_{wt}$. To construct pTrc-fruR$_{wt}$ and pTrc-fruR$_{mut}$, the *fruR*$_{wt}$ and *fruR*$_{mut}$ genes were amplified from the genome of *E. coli* W3110 and HDH6-D12 and ligated into pTrc99a vector according to the previous description.

Enzymatic Activity Analysis of AHAS. The enzyme activity of acetohydroxy acid synthase (AHAS) was determined using the published assay.[49] Both *ilvH* and *ilvI* were separately ligated into the pET28a vector and expressed in *E. coli* BL21. The crude enzyme extract was added to 1 mL of reaction buffer containing 100 mM sodium pyruvate, 0.2 mM thiamine pyrophosphate, 100 μM flavin adenine dinucleotide (FAD), and 10 mM $MgCl_2$. The reaction was initiated by addition of 100 μL of crude extract to 900 μL of reaction mixture, and then the reaction mixture was incubated at 37 °C for 20 min. The reaction was terminated by addition of 100 μL of 3 M H_2SO_4. The generated acetoin was measured by addition of 1 mL of 0.5% creatine and 1 mL of α-naphthol solution, incubation at 65 °C for 20 min, and measurement of the optical density at 525 nm. The AHAS activity was defined as the amount of enzyme required for the formation of 1 mole of 2-aceto-2-hydroxybutyrate per minute at 37 °C.

Quantitative Real-Time PCR Analysis. A single colony was isolated from a freshly streaked selective plate and inoculated in 5 mL of LB medium at 37 °C overnight. Cells were transferred into 5 mL of LB medium at a ratio of 1:100 and induced by 1 mM IPTG when the OD_{600} reached 0.6. Subsequently cells were collected by centrifugation at 12000*g* and then resuspended in lysis buffer (Tiangen, China). RNA extraction was processed according to the manual (Tiangen, China), and the first-strand cDNAs were synthesized using the PrimerScript RT reagent kit (Takara, Japan). cDNA was diluted into a 5-fold volume of ddH_2O, and 1 μL of this cDNA dilution was used for the following real-time PCR analysis. The reaction system consisted of 1.0 μL of forward primer (10 μM), 1.0 μL of reverse primer (10 μM), 1.0 μL of cDNA sample, 8.5 μL of dH_2O, and 10 μL of SYBR Premix Ex *Taq*II (FastStart Universal SYBR Green Master, Rox, USA). The real-time PCR analysis was carried out by employing the LightCycler system (LightCycler, Roche, USA) under the following conditions: 95 °C for 10 min, followed by 45 cycles of 95 °C for 10 s, 60 °C for 10 s, and 72 °C for 20 s. At the end of the reaction, the dissociation curve was analyzed by raising the reaction temperature from 60 to 95 °C.

■ ASSOCIATED CONTENT

Supporting Information

The Supporting Information is available free of charge on the ACS Publications website at DOI: 10.1021/acssynbio.6b00328.

Characterization of five biosensor plasmids in response to addition of increasing amounts of Phe-Phe to the medium (Figure S1); growth conditions of five L-Phe-producing strains (Figure S2); lethality curve of strains treated for different mutation times (Figure S3); determination of the optimal concentration of streptomycin for HTS of L-Phe hyperproducing strains on agar plates (Figure S4); L-Phe concentrations in fermentation medium measured by fluorescence assay and HPLC assay (Figure S5); L-Phe production of strains obtained by FACS selection or by random selection (Figure S6); plasmid profile of pUC18-yddG$_{wt}$ (Figure S7); plasmid profile of pTrc-fruR$_{wt}$ (Figure S8); variation in the translation levels of genes related to central metabolism for hyperproducing strain HDH6-D12 upon addition of different concentrations of phenylalanine in culture (Figure S9); diagrammatic sketch of the primers for dsRNA (Figure S10); strains and plasmids used in this study (Table S1); primers used in this study (Table S2); sequences of the promoter regions of the four biosensors (Table S3); list of SNPs in the HDH6-D12 strain (Table S4) (PDF)

■ AUTHOR INFORMATION

Corresponding Author

*E-mail: zhang_dw@tib.cas.cn.

ORCID

Dawei Zhang: 0000-0002-5857-394X

Author Contributions

Y.L., J.S., and D.Z. designed the experiments and wrote the manuscript. Y.L., Y.Z., D.D., and Y.X. performed the experiments and analyzed the data.

Notes

The authors declare no competing financial interest.

■ ACKNOWLEDGMENTS

The authors are grateful for financial support from the State Key Development 973 Program for Basic Research of China (2013CB733601), the National Natural Science Foundation of China (31370089), the Key Projects in the Tianjin Science & Technology Pillar Program (11ZCZDSY08600), and the Natural Science Foundation of Tianjin City (CN) (16JCYBJC23500). We also thank Lothar Eggeling (Forschungszentrum Jülich GmbH, Germany) for the plasmid pSenlys and Xueming Zhao (Tianjin University, China) for the plasmid pREDCas9.

■ REFERENCES

(1) Redding-Johanson, A. M., Batth, T. S., Chan, R., Krupa, R., Szmidt, H. L., Adams, P. D., Keasling, J. D., Lee, T. S., Mukhopadhyay,

DOI: 10.1021/acssynbio.6b00328
ACS Synth. Biol. 2017, 6, 837−848

A., and Petzold, C. J. (2011) Targeted proteomics for metabolic pathway optimization: application to terpene production. *Metab. Eng. 13*, 194−203.
(2) Blankschien, M. D., Clomburg, J. M., and Gonzalez, R. (2010) Metabolic engineering of Escherichia coli for the production of succinate from glycerol. *Metab. Eng. 12*, 409−419.
(3) Shen, C. R., and Liao, J. C. (2008) Metabolic engineering of Escherichia coli for 1-butanol and 1-propanol production via the keto-acid pathways. *Metab. Eng. 10*, 312−320.
(4) Liu, Y., Liu, L., Shin, H. D., Chen, R. R., Li, J., Du, G., and Chen, J. (2013) Pathway engineering of Bacillus subtilis for microbial production of N-acetylglucosamine. *Metab. Eng. 19*, 107−115.
(5) Xu, Y., Chu, H., Gao, C., Tao, F., Zhou, Z., Li, K., Li, L., Ma, C., and Xu, P. (2014) Systematic metabolic engineering of Escherichia coli for high-yield production of fuel bio-chemical 2,3-butanediol. *Metab. Eng. 23*, 22−33.
(6) Dietrich, J. A., McKee, A. E., and Keasling, J. D. (2010) High-throughput metabolic engineering: advances in small-molecule screening and selection. *Annu. Rev. Biochem. 79*, 563−590.
(7) Rogers, J. K., Taylor, N. D., and Church, G. M. (2016) Biosensor-based engineering of biosynthetic pathways. *Curr. Opin. Biotechnol. 42*, 84−91.
(8) Yu, H., Tyo, K., Alper, H., Klein-Marcuschamer, D., and Stephanopoulos, G. (2008) A high-throughput screen for hyaluronic acid accumulation in recombinant Escherichia coli transformed by libraries of engineered sigma factors. *Biotechnol. Bioeng. 101*, 788−796.
(9) Santos, C. N. S., Xiao, W. H., and Stephanopoulos, G. (2012) Rational, combinatorial, and genomic approaches for engineering L-tyrosine production in Escherichia coli. *Proc. Natl. Acad. Sci. U. S. A. 109*, 13538−13543.
(10) Wang, C., Leffler, S., Thompson, D. H., and Hrycyna, C. A. (2005) A general fluorescence-based coupled assay for S-adenosylmethionine-dependent methyltransferases. *Biochem. Biophys. Res. Commun. 331*, 351−356.
(11) Yang, J., Seo, S. W., Jang, S., Shin, S. I., Lim, C. H., Roh, T. Y., and Jung, G. Y. (2013) Synthetic RNA devices to expedite the evolution of metabolite-producing microbes. *Nat. Commun. 4*, 1413.
(12) Wang, B., Barahona, M., and Buck, M. (2015) Amplification of small molecule-inducible gene expression via tuning of intracellular receptor densities. *Nucleic Acids Res. 43*, 1955−1964.
(13) Galvao, T. C., and de Lorenzo, V. (2006) Transcriptional regulators a la carte: engineering new effector specificities in bacterial regulatory proteins. *Curr. Opin. Biotechnol. 17*, 34−42.
(14) Binder, S., Schendzielorz, G., Stabler, N., Krumbach, K., Hoffmann, K., Bott, M., and Eggeling, L. (2012) A high-throughput approach to identify genomic variants of bacterial metabolite producers at the single-cell level. *Genome biology 13*, R40.
(15) Mustafi, N., Grünberger, A., Kohlheyer, D., Bott, M., and Frunzke, J. (2012) The development and application of a single-cell biosensor for the detection of l-methionine and branched-chain amino acids. *Metab. Eng. 14*, 449−457.
(16) Raman, S., Rogers, J. K., Taylor, N. D., and Church, G. M. (2014) Evolution-guided optimization of biosynthetic pathways. *Proc. Natl. Acad. Sci. U. S. A. 111*, 17803−17808.
(17) Krueger, M., Scholz, O., Wisshak, S., and Hillen, W. (2007) Engineered Tet repressors with recognition specificity for the tetO-4C5G operator variant. *Gene 404*, 93−100.
(18) Xu, P., Wang, W., Li, L., Bhan, N., Zhang, F., and Koffas, M. A. (2014) Design and kinetic analysis of a hybrid promoter-regulator system for malonyl-CoA sensing in Escherichia coli. *ACS Chem. Biol. 9*, 451−458.
(19) Tang, S. Y., Qian, S., Akinterinwa, O., Frei, C. S., Gredell, J. A., and Cirino, P. C. (2013) Screening for enhanced triacetic acid lactone production by recombinant Escherichia coli expressing a designed triacetic acid lactone reporter. *J. Am. Chem. Soc. 135*, 10099−10103.
(20) Dietrich, J. A., Shis, D. L., Alikhani, A., and Keasling, J. D. (2013) Transcription factor-based screens and synthetic selections for microbial small-molecule biosynthesis. *ACS Synth. Biol. 2*, 47−58.
(21) Tang, S. Y., and Cirino, P. C. (2011) Design and application of a mevalonate-responsive regulatory protein. *Angew. Chem., Int. Ed. 50*, 1084−1086.
(22) Tang, S. Y., Fazelinia, H., and Cirino, P. C. (2008) AraC regulatory protein mutants with altered effector specificity. *J. Am. Chem. Soc. 130*, 5267−5271.
(23) de Las Heras, A., and de Lorenzo, V. (2011) Cooperative amino acid changes shift the response of the sigma(5)(4)-dependent regulator XylR from natural m-xylene towards xenobiotic 2,4-dinitrotoluene. *Mol. Microbiol. 79*, 1248−1259.
(24) Pittard, J., Camakaris, H., and Yang, J. (2005) The TyrR regulon. *Mol. Microbiol. 55*, 16−26.
(25) Lawley, B., Fujita, N., Ishihama, A., and Pittard, A. J. (1995) The Tyrr Protein of Escherichia-Coli Is a Class-I Transcription Activator. *J. Bacteriol. 177*, 238−241.
(26) Trotschel, C., Deutenberg, D., Bathe, B., Burkovski, A., and Kramer, R. (2005) Characterization of methionine export in Corynebacterium glutamicum. *J. Bacteriol. 187*, 3786−3794.
(27) Yang, J., Hwang, J. S., Camakaris, H., Irawaty, W., Ishihama, A., and Pittard, J. (2004) Mode of action of the TyrR protein: repression and activation of the tyrP promoter of Escherichia coli. *Mol. Microbiol. 52*, 243−256.
(28) Andrews, A. E., Dickson, B., Lawley, B., Cobbett, C., and Pittard, A. J. (1991) Importance of the position of TYR R boxes for repression and activation of the tyrP and aroF genes in Escherichia coli. *J. Bacteriol. 173*, 5079−5085.
(29) Lee, K. H., Park, J. H., Kim, T. Y., Kim, H. U., and Lee, S. Y. (2007) Systems metabolic engineering of Escherichia coli for L-threonine production. *Mol. Syst. Biol. 3*, 149.
(30) Mccaman, M. W., and Robins, E. (1962) Fluorimetric method for the determination of phenylalanine in serum. *J. Lab. Clin. Med. 59*, 885−890.
(31) Li, Y., Lin, Z., Huang, C., Zhang, Y., Wang, Z., Tang, Y. J., Chen, T., and Zhao, X. (2015) Metabolic engineering of Escherichia coli using CRISPR-Cas9 meditated genome editing. *Metab. Eng. 31*, 13−21.
(32) Bizouarn, T., Althage, M., Pedersen, A., Tigerstrom, A., Karlsson, J., Johansson, C., and Rydstrom, J. (2002) The organization of the membrane domain and its interaction with the NADP(H)-binding site in proton-translocating transhydrogenase from E-coli. *Biochim. Biophys. Acta, Bioenerg. 1555*, 122−127.
(33) Shi, A., Zhu, X., Lu, J., Zhang, X., and Ma, Y. (2013) Activating transhydrogenase and NAD kinase in combination for improving isobutanol production. *Metab. Eng. 16*, 1−10.
(34) Bastian, S., Liu, X., Meyerowitz, J. T., Snow, C. D., Chen, M. M., and Arnold, F. H. (2011) Engineered ketol-acid reductoisomerase and alcohol dehydrogenase enable anaerobic 2-methylpropan-1-ol production at theoretical yield in Escherichia coli. *Metab. Eng. 13*, 345−352.
(35) Kaplun, A., Vyazmensky, M., Zherdev, Y., Belenky, I., Slutzker, A., Mendel, S., Barak, Z., Chipman, D. M., and Shaanan, B. (2006) Structure of the regulatory subunit of acetohydroxyacid synthase isozyme III from Escherichia coli. *J. Mol. Biol. 357*, 951−963.
(36) Vyazmensky, M., Sella, C., Barak, Z., and Chipman, D. M. (1996) Isolation and characterization of subunits of acetohydroxy acid synthase isozyme III and reconstitution of the holoenzyme. *Biochemistry 35*, 10339−10346.
(37) Doroshenko, V., Airich, L., Vitushkina, M., Kolokolova, A., Livshits, V., and Mashko, S. (2007) YddG from Escherichia coli promotes export of aromatic amino acids. *FEMS Microbiol. Lett. 275*, 312−318.
(38) Sinha, J., Reyes, S. J., and Gallivan, J. P. (2010) Reprogramming bacteria to seek and destroy an herbicide. *Nat. Chem. Biol. 6*, 464−470.
(39) Fowler, C. C., Brown, E. D., and Li, Y. (2010) Using a riboswitch sensor to examine coenzyme B(12) metabolism and transport in E. coli. *Chem. Biol. 17*, 756−765.
(40) Saito, H., Fujita, Y., Kashida, S., Hayashi, K., and Inoue, T. (2011) Synthetic human cell fate regulation by protein-driven RNA switches. *Nat. Commun. 2*, 160.

DOI: 10.1021/acssynbio.6b00328
ACS Synth. Biol. 2017, 6, 837−848

(41) Becker, J., and Wittmann, C. (2012) Systems and synthetic metabolic engineering for amino acid production - the heartbeat of industrial strain development. *Curr. Opin. Biotechnol. 23*, 718−726.
(42) Liu, S. P., Zhang, L., Mao, J., Ding, Z. Y., and Shi, G. Y. (2015) Metabolic engineering of Escherichia coli for the production of phenylpyruvate derivatives. *Metab. Eng. 32*, 55−65.
(43) Zhou, H., Liao, X., Wang, T., Du, G., and Chen, J. (2010) Enhanced l-phenylalanine biosynthesis by co-expression of pheA(fbr) and aroF(wt). *Bioresour. Technol. 101*, 4151−4156.
(44) Rodriguez, A., Martinez, J. A., Flores, N., Escalante, A., Gosset, G., and Bolivar, F. (2014) Engineering *Escherichia coli* to overproduce aromatic amino acids and derived compounds. *Microb. Cell Fact. 13*, 126.
(45) Yamamoto, K., and Ishihama, A. (2006) Characterization of copper-inducible promoters regulated by CpxA/CpxR in Escherichia coli. *Biosci., Biotechnol., Biochem. 70*, 1688−1695.
(46) Man, T. K., Pease, A. J., and Winkler, M. E. (1997) Maximization of transcription of the serC (pdxF)-aroA multifunctional operon by antagonistic effects of the cyclic AMP (cAMP) receptor protein-cAMP complex and Lrp global regulators of Escherichia coli K-12. *J. Bacteriol. 179*, 3458−3469.
(47) Tatarko, M., and Romeo, T. (2001) Disruption of a global regulatory gene to enhance central carbon flux into phenylalanine biosynthesis in Escherichia coli. *Curr. Microbiol. 43*, 26−32.
(48) Ding, D., Liu, Y., Xu, Y., Zheng, P., Li, H., Zhang, D., and Sun, J. (2016) Improving the Production of L-Phenylalanine by Identifying Key Enzymes Through Multi-Enzyme Reaction System in Vitro. *Sci. Rep. 6*, 32208.
(49) Vyazmensky, M., Sella, C., Barak, Z., and Chipman, D. M. (1996) Isolation and characterization of subunits of acetohydroxy acid synthase isozyme III and reconstitution of the holoenzyme. *Biochemistry 35*, 10339−10346.

DOI: 10.1021/acssynbio.6b00328
ACS Synth. Biol. 2017, 6, 837−848